

# On Experimental Confirmation of the Corrections to the Fermi's golden rule

Kenzo Ishikawa<sup>1,2</sup>, Osamu Jinnouch<sup>3</sup>, Arisa Kubota<sup>3</sup>,  
Terrey Sloan<sup>4</sup>, Takuya H. Tatsuishi<sup>1</sup>, and Risa Ushiosa<sup>3</sup>

<sup>1</sup>*Department of Physics, Faculty of Science,  
Hokkaido University, Sapporo 060-0810, Japan*

<sup>2</sup>*Natural Science center , Keio University , Hiyoshi Japan*

<sup>3</sup>*Department of Physics, Faculty of Science  
Tokyo Institute of Technology, Tokyo , Japan and*

<sup>4</sup>*Department of Physics, Faculty of Science  
Lancaster University, Lancaster , UK*

(Dated: November 27, 2024)

## Abstract

Standard calculations by the Fermi's Golden Rule involve approximations. These approximations could lead to deviations from the predictions of the standard model as discussed in another paper. In this paper we propose experimental searches for such deviations in the two photon spectra from the decay of the neutral pion in the process  $\phi \rightarrow \pi^+\pi^-\pi^0$  and in the annihilation of the positron from nuclear  $\beta$  decay.

## I. THE CORRECTION TO THE FERMI'S GOLDEN RULE

In interacting many-body system described by a Hamiltonian  $H_0 + H_1$ , a state evolves with a Schrödinger equation. One particle state is specified by the momentum and non-interacting energy defined by  $H_0$ . A transition by  $H_1$  has been studied by the Fermi's golden rule. Although these transitions have been paid attention from researchers, those that do not conserve the energy often arise, when the approximations are taken into account. The Schrödinger equation includes these approximations, which affect transitions of any states. Surprisingly, a correction term beyond the Fermi's golden rule emerges. The correction becomes manifest in a transition of a finite time interval, in which that reveals different dependence on the time interval and on the energy difference. The correction terms would have been identified from experimental data. However it is not simple as was naively thought due to several reasons. One reason is that those signals that are caused by the corrections terms are similar to those of experimental background. In majority cases, they were considered as the background, and discarded. Another reason is on a difficulty to find the absolute value of the physical quantity in experiments, because the data is always modified by an efficiency of detector. The transition rate describes average behavior [1, 2] of the process, and the correction terms give dominant contribution to rapidly changing processes. Direct observation of these events might give signals of the correction terms, but has not been possible up to the present. In general it is difficult to separate these from the real background.

Accordingly the correction terms was not a major concern from researchers. Nevertheless, the correction is one part of the total probability and contributes to natural phenomena. Fitting these experiments in approximate way without the correction term might be possible and viable for certain period. However, that should lead serious inconsistency or fatal outcome at later time, which must be avoided. It is urgent to confirm an existence of the correction term with simple and clean experiments.

Two photon processes of the neutral pion and the positron annihilation supply precise information on the transitions and can be candidates. The rates have theoretically been well-understood, and determined from the various experiments, in which the background have been subtracted. There are subtlety on the background subtraction, and a signal of the correction term has been insignificant. The correction terms are computed in a separate

paper [3] and are found sizable. Due to their unusual properties, which will be presented later, it is not an easy task to disentangle them from the real background. Nevertheless, they give universal contributions to the phenomena. It will be shown that these are feasible in  $\phi$ -factory for the pion and in nuclear beta decays for the positron.

The neutral pion,  $\pi^0$ , is the lightest hadron composed of the quark and anti-quark and supplies many informations on particle physics [4]. The rate of  $\pi^0$  decay to two photons [5, 6] is proportional to the number of the color  $N_c$  [7, 8], and the measurement on life time  $\tau = 10^{-16}$  seconds determines  $N_c = 3$ . Despite of this remarkable success, the average life-time obtained from various methods [9] has large uncertainty of about 10 per cent. Accordingly, K-meson decays to two or three pions have also large uncertainties [4]. A large uncertainty arises also in the decay of para-positronium, which is a bound state of the electron and positron in Quantum Electrodynamics (QED). Its properties and transition rates are understood well, but the precision is not very good. The large uncertainty of the experimental values may suggest a fundamental problem on the transition probability.

We find the many body wave function  $|\Psi\rangle$  composed of normalized states from the Schrödinger equation

$$i\hbar\frac{\partial}{\partial t}|\Psi\rangle = (H_0 + H_{\text{int}})|\Psi\rangle, \quad (1)$$

, where  $H_0$  and  $H_{\text{int}}$  are the free and interaction parts, and compute the rigorous transition amplitude. Hereafter we employ the natural units  $\hbar = c = 1$  unless otherwise stated. A transition probability from a state  $|i, 0\rangle$  at  $t = 0$  to a state  $|f, T\rangle$  at  $t = T$  is determined by the von Neumann's fundamental principle of the quantum mechanics (FQM) as ,  $P(T) = |\langle f, T | i, 0 \rangle|^2$ , for normalized states. For  $P(T) \ll 1$ , the average rate  $\Gamma = \frac{P(T) - P(T_i)}{T - T_i}$  between a small  $T_i$  and a large  $T$ , is given from a ratio of fluxes of out-going waves over that of incident waves and is in agreement with that derived from the golden rule for the final state of continuous spectrum. In these standard calculations, the plane waves and the interaction that switches off adiabatically (ASI) are used. Although, this value has been used in the majority of the processes, experiments are made at the finite time intervals and the value is measured without average.

Theoretical values under these conditions are necessary.

Stueckelberg studied this problem sometime ago and found that the transition amplitudes of the plane waves for finite-time interval lead a divergence [10] even in the tree level.

This is unconnected with the ultraviolet divergences due to the intermediate states but to non-normalized initial and final states. It is possible to avoid this difficulty by using the normalized states. Those computed in the previous paper [3] are applied to experiments.

$P(T)$  at a large  $T$  is the sum,

$$P(T) = \Gamma T + P^{(d)}, \quad P^{(d)} = P(T_i) - \Gamma T_i. \quad (2)$$

$T_i$  is determined by a time that the initial wave packets separates. This is determined by  $\sqrt{\sigma_i}$ , where  $\sigma_i$  is the spatial size of the initial wave. At  $\Gamma T_i < 1$ , and at  $T > T_i$ ,  $P^{(d)}$  is constant.

$\Gamma$ , is computed with the standard S-matrix  $S[\infty]$  under ASI [11–13], but  $P^{(d)}$  is computed with the wavefunctions following FQM [14–17]. A rigorous probability will be obtained without facing the difficulty raised by Stueckelberg by using the wave packets instead of the plane waves.

Experimental proof of  $P^{(d)}$  in the neutral pion decay, the positronium decay, and the positron annihilations are studied. Two photon decays of a para-positronium is almost equivalent to the neutral pion decay. Their systematic analyses are presented. It will be shown that the unique properties derived from the probability  $\Gamma T + P^{(d)}$  can be confirmed experimentally.

The paper is organized as follows: In Section 2, the pion decay is analyzed and in Section 3, the positron annihilation is analyzed. In Section 4 the wave packets sizes and relevant parameters are estimated. In Section 5 the experiments are studied and summary and prospects are presented. Appendix A is devoted to various formula and Appendix B is devoted to a method for entanglement of the accidental background.

## II. TWO PHOTON DECAY OF THE NEUTRAL PION

The interaction of a neutral pion or a para-positronium with two photons are derived from the triangle diagram of the quark or the electron as  $L_{\text{int}} = -g \varphi \epsilon_{\mu\nu\rho\sigma} F^{\mu\nu} F^{\rho\sigma}$  in which the coupling for the pion is  $g = \frac{\alpha}{4\pi f_\pi}$  is almost constant from the confining mechanism and is related with the  $\pi\gamma\gamma$  coupling [7, 8]. For the positronium, the binding energy is small and the coupling varies with the momentum, which will be ignored for a while. Substituting this to Eq.(1), we have the transition amplitude for an initial state of a central momentum and

position into two photons

$$\mathcal{M} = \int_{T_\pi}^{T_\gamma} dt \int d^3x \langle K_1, X_1; K_2, X_2 | H_{\text{int}}(x) | P_\pi, X_\pi \rangle \quad (3)$$

Gaussian wave packet [14],[18],[19],[20] satisfies the minimum uncertainty, which is idealistic for studying a transition of finite-time interval, and is used in majority of places. Non-Gaussian form is also physically relevant and studied later. Wave packets of the size  $\sigma_i$ , the central momentum, and the central position are used throughout this paper, where  $i = 1, 2$ ,  $E_A = \sqrt{P_A^2 + m_A^2}$ ,  $E(K_i) = |K_i|$ , and  $\vec{V}_A = \frac{\vec{P}_A}{E_A}$  is the group velocity of the momentum  $\vec{P}_A$ . Throughout this paper, the upper-case roman letters  $A, B, \dots$  run for  $\pi, 1, 2$  so that e.g.  $\sum_A$  stands for  $\sum_{A=\pi,1,2}$ , etc. An imaginary part is added to the energy of the unstable initial state according to Ref. [21, 22]; see also e.g. Ref. [11] for a review is taken. Integration over the space position leads to a Gaussian function in the momentum difference, and that over the time leads to <sup>1</sup>

$$\mathcal{M} = N_0(\vec{X}_i) \epsilon_{\mu\nu\rho\sigma} \epsilon^\mu(K_1) K_1^\nu \epsilon^\rho(K_2) K_2^\sigma e^{-\frac{\sigma_s}{2}(\delta P)^2} G(\delta\omega), \quad (4)$$

where  $N_0(\vec{X}_i)$  shows a dependence on the positions,  $\delta P = P_\pi - K_1 - K_2$ ,  $\delta\omega = E_\pi - E_1 - E_2 - \vec{V}_0 \delta P$ , and  $\sigma_s = \left(\sum_A \frac{1}{\sigma_A}\right)^{-1}$ ,  $G(\delta\omega)$  is expressed with the error function  $\text{erf}(x+iy)$ . Their explicit forms are given in [3]. The transition probability is written as,

$$P = \frac{1}{2} \int d^3X_1 d^3X_2 \frac{d^3K_1}{(2\pi)^3} \frac{d^3K_2}{(2\pi)^3} \left| N_0(\vec{X}_i) \right|^2 2 (K_1 \cdot K_2)^2 e^{-\sigma_s(\delta P)^2} |G(\delta\omega)|^2, \quad (5)$$

As is shown in Ref. [3] in details,  $G(\delta\omega)$  depends on an intersection of the trajectories determined by the positions of  $\vec{X}_i; i = 1, 2$ . If they intersect outside of the material, the interaction does not occur and the amplitude vanishes. If that is inside of the material, the interaction occurs. This is a bulk region. In the boundary region, the interaction occurs partly. This is the boundary region.

The integration in the bulk is proportional to the time interval due to the translational invariance along the initial momentum, and that in the boundary is proportional to the width of the boundary region,  $\sigma_t$ , which depends on the wave packet size and the velocity variation,  $\sigma_t = \frac{\sigma_s}{\Delta V^2}$ . The derivation is given in [3]

---

<sup>1</sup> We have put the central momentum  $K_i$  in the polarization  $\epsilon^\mu$  and in the derivative interaction. See Ref. [17] for its justification.

The momentum distribution is written as a sum of two terms,

$$\frac{dP}{d^3K_1 d^3K_2} = 2 (K_1 \cdot K_2)^2 e^{-\sigma_s(\delta P)^2} \sum_{k=\text{bulk},\text{boundary}} P_0^k |G^k(\delta\omega)|^2, \quad (6)$$

where

$$P_0^k = \begin{cases} g^2 2^{-6} (\sigma_\pi)^{-3/2} (E_\pi E_1 E_2)^{-1} C \tau_\pi \left(1 - e^{-\frac{T}{\tau_\pi}}\right) & \text{for bulk,} \\ g^2 2^{-6} (\sigma_\pi)^{-3/2} (E_\pi E_1 E_2)^{-1} C \sqrt{2\sigma_t} & \text{for boundary,} \end{cases} \quad (7)$$

where  $T = T_\gamma - T_\pi$ ,  $C$  is a constant of energy dimension  $E^1$  and depends on the wave packet parameters. The squares of  $G(\delta\omega)$  in the asymptotic region is,

$$|G(\delta\omega)|^2 = e^{\frac{\sigma_t}{4\tau_\pi}} \times \begin{cases} \frac{e^{-\frac{(T_0^R - T_\pi)^2}{\sigma_t} + \frac{T_0^R - T_\pi}{\tau_\pi}}}{(T_0^R - \frac{T_\gamma}{\sigma_t} - \frac{1}{2\tau_\pi})^2 + (\delta\omega)^2} & \text{from boundary } (\frac{\sigma_t}{2}\delta\omega^2 \gg 1), \\ 2\pi\sigma_t e^{-\sigma_t(\delta\omega)^2} & \text{from bulk } (\frac{\sigma_t}{2}\delta\omega^2 \ll 1), \end{cases} \quad (8)$$

where  $T_0^R$  is the time that the wave packets intersect. The bulk term decreases rapidly with  $\delta\omega$  and the boundary term decreases slowly with an inverse power of the energy difference.

In the decay of the high energy pion of  $p_\pi = (E_\pi, 0, 0, p_\pi)$ , the momenta of the final states are almost parallel to the pion. In the boundary term,  $|G(\delta\omega)|^2$  decreases slowly at  $K_i \rightarrow \infty$ , and leads a large contribution to the probability.

In the transition, the total energy is conserved but the kinetic energy is partly violated. The bulk contribution is narrow in the kinetic energy, and reveals the golden rule. The boundary contribution is broad in the kinetic energy, and reveals the correction term. The deviation of the kinetic energy from the total energy is the interaction energy  $V_{\text{int}} = \langle \Psi | H_{\text{int}} | \Psi \rangle$ . The coupling strength  $g$  can be treated as constant for the golden rule, where  $k_{\gamma_i} \cdot k_{\gamma_{i'}} \ll m_q$ . However, the boundary term is spread in wide kinetic region of  $k_{\gamma_i} \cdot k_{\gamma_{i'}}$ , which includes a region  $k_{\gamma_i} \cdot k_{\gamma_{i'}} \gg m_q^2$ . There, this coupling strength becomes a function of  $k_{\gamma_i} \cdot k_{\gamma_{i'}}$ ,  $g(k_{\gamma_i} \cdot k_{\gamma_{i'}})$ , behaving as

$$g(k_{\gamma_i} \cdot k_{\gamma_{i'}}) = g \frac{m_q^2}{2k_{\gamma_i} \cdot k_{\gamma_{i'}}} \quad (9)$$

[23]. Here  $m_q$  is the composite quark mass of a magnitude around  $\frac{m_p}{3}$ , where  $m_p$  is the proton's mass. Thus  $P^{(d)}$  becomes maximum at around  $k_{\gamma_i} \cdot k_{\gamma_{i'}} \approx \frac{m_p^2}{2}$ . Its magnitude is proportional to the proton's mass. This behavior shows that the average interaction energy  $\langle |H_{\text{int}}| \rangle$  is the order of the proton's rest energy,  $m_p$ .

For a high energy pion, the initial and final waves overlap in wide area for photons propagating in the parallel direction to the pion. The boundary region becomes large in size, and gives large contribution to the probability.

### III. POSITRON ANNIHILATION

Positron and electron are described by the field  $\psi(x)$ , and photon is by  $A_\mu(x)$  in the Quantum Electrodynamics, and the interaction is  $e\bar{\psi}(x)\gamma_\mu\psi(x)A^\mu(x)$ . The para-positronium decay and the free positron annihilation are derived from this interaction. The former one is also expressed by an effective interaction equivalent to the pion-two photon interaction. The latter one is described by the 2nd order perturbative expansion with respect to the above interaction.  $P(T)$  in these decays are studied.

#### A. Para-positronium decay

Para-positronium is even in the charge conjugation and decays to two photons. The formula of decay probability Eq.(6) is applied after changing parameters with suitable ones. The average lifetime of the Para-positronium is much longer than that of the pion and the wave packet size is also longer. The positronium decays and positron annihilation in porous material, which are composed of small holes and many boundary regions, are analyzed. We will see that the boundary term is enhanced.

#### B. Free positron annihilation

The annihilation amplitude of the free positron and the free electron at rest for those of the central values of momentum and position,

$$\chi_{e_i} = (\vec{p}_{e_i}, \vec{X}_{e_i}, \sigma_{e_i}), \chi_{\gamma_i} = ((\vec{p}_{\gamma_i}, \vec{X}_{\gamma_i}, \sigma_{\gamma_i})) \quad (10)$$

for the photons, the electron, and the positron,

$$\mathcal{M} = \langle \chi_{\gamma_1}; \chi_{\gamma_2} | \int_0^T dx_1 \int_0^{t_1} dx_2 H_{int}(x_1) H_{int}(x_2) | \chi_{e_1}, \chi_{\bar{e}_2} \rangle, \quad (11)$$

where  $T$  is the time interval that the positron crosses a grain of the target. The integrations over the coordinates  $\vec{x}_i$ , and over the momentum  $\vec{q}$  for the intermediate state are made using Gaussian integrations.

The integration over times give the bulk and boundary terms, and lead the amplitude to be written as Eq.(4). Substituting these, we have the momentum distribution

$$\begin{aligned} \frac{1}{TL^3} \frac{dP}{d^3k_1 d^3k_2} &= \frac{2}{m^2} \left( 1 + \frac{1}{4}(1 - \cos \theta) + \frac{1}{2} \left( \frac{m}{E_{\gamma_1}} + \frac{m}{E_{\gamma_2}} \right) \right) \\ & [e^{-\sigma_s(\delta P)^2} (P_0^{bulk} |G_{bulk}(\delta\omega)|^2 + P_0^{bt} |G_{boundary(t)}(\delta\omega)|^2) \\ & + P_0^{bs} e^{-\sigma_s(\delta P)^2} |G_{boundary(s)}(\delta\omega)|^2], \end{aligned} \quad (12)$$

where Eqs.(A22) and (A12) are substituted, and

$$P_0^{bulk} = (E_{e^+} E_{\gamma_1} E_{\gamma_2})^{-1} C \quad \text{bulk}, \quad (13)$$

$$P_0^{b(t)} = (E_{e^+} E_{\gamma_1} E_{\gamma_2})^{-1} C \frac{\sqrt{2\sigma_t}}{T} \quad \text{boundary in time}, \quad (14)$$

$$P_0^{b(s)} = (E_{e^+} E_{\gamma_1} E_{\gamma_2})^{-1} C \frac{\sqrt{2\sigma_t 2\sigma_s}}{TL} \quad \text{boundary in space}, \quad (15)$$

where  $C$  is the constant [3]. In silica powder, this size is semi-microscopic of order few nano meter, and almost the same or slightly larger than  $\sqrt{\sigma_\gamma}$ . In the present situation, the target is composed of silica particles of  $L = 7$  nano meter, and it is reasonable to assume the ratios  $\frac{\sqrt{2\sigma_s}}{L}$  and  $\frac{\sqrt{2\sigma_t}}{T}$  are  $\frac{1}{10} - \frac{1}{100}$ . The positron energy is  $E_{e^+} = m_e$  with the energy uncertainty of 10 per cent. The spectrum of the boundary term is of the universal form but its magnitude has uncertainties due to the uncertainties on the wave packets. This ambiguity could be studied by a light scattering of the silica powder [24].

#### IV. INITIAL AND FINAL STATES

We apply the decay probability Eq. (6) to the neutral pion in the process

$$e^+ + e \rightarrow \phi \rightarrow \pi^+ + \pi^- + \pi^0 \quad (16)$$

, and that of the positron Eq.(12) in the process

$${}^{22}\text{Na} \rightarrow {}^{22}\text{Ne}^* + e^+ + \nu, {}^{22}\text{Ne}^* \rightarrow {}^{22}\text{Ne} + \gamma. \quad (17)$$

The former experiment is made in a high energy laboratory and the latter experiment is made in a low-energy laboratory.

## A. Wave packet shape and size

The total transition rate  $\Gamma$  derived from Eqs. (6) and (12) is independent of the wave packet parameters. This is consistent with the general theorem given by Stodolsky [25] [26] [27] [28] on stationary physical quantities. This theorem, however, is not applied to a non-stationary quantity such as  $P^{(d)}$ . In fact  $P^{(d)}$  derived from Eqs. (6) and (12) depend on the forms and sizes of the wave packets. Up to here the Gaussian wave packet, which decreases exponentially in the position and the momentum and satisfies the minimum uncertainty  $\delta x \delta p = \hbar$ , and  $\delta p = 0$  for  $\delta x = \infty$  is used. This is idealistic for studying the transition for a finite time interval. Other wave packet satisfying  $\delta x \delta p \geq \hbar$  is shown to lead almost equivalent results.  $\sigma_\pi$ ,  $\sigma_\gamma$ , and  $\sigma_{\bar{e}}$  stand for  $\sigma_s$  of the pion, photon, and positron.

These particles interact with microscopic objects in matters and cause the final states to be produced, from which a number of the events and the probability are determined. Accordingly the packet parameters in our formula are determined by these states in matter. This method has been shown valid in [14–17], and in quantum transition of two atoms in an energy transfer process in photosynthesis [29].

### 1. Sizes of wave functions : $\pi^0$

$\sigma_{\pi_0}$

In order for the electron and the positron to produce a  $\phi$  meson, they are accelerated from average electron momentum in matter, which is less than  $\frac{1}{10^{-10}\text{Meter}}$ . A relaxation time for these electron and positron in matter, beyond which these lose coherence due to environmental effect is around  $10^{-14}$  second, which corresponds to the mean free path  $3 \times 10^{-6}$  Meters for the speed of light, and slightly shorter at lower energy.  $10^{-14}$  second and  $10^{-7}$  Meters for the spatial electron sizes in matter are used. The positron is produced by the electron collision with matter, and the length is the same as that of the electrons. During their acceleration, the time interval that the wave packets pass through at a spatial position is kept unchanged. Although the amplitude of three pions, which is described by the intermediate  $\phi$  meson of the Breit-Wigner form of the energy width of few MeV, peaks around the central energy, if the initial state has a fixed energy, each pion can have infinitesimal energy uncertainty. Accordingly the width of the  $\phi$  meson is related neither

to the uncertainty of the pion's energy nor to the pion's wave packet size. Nevertheless, the above relaxation time of the electron and positron results to an uncertainty of the three pion's energy, few meV. Thus the energy uncertainty of  $\pi^0$  is governed by the relaxation time. That leads  $3 \times 10^{-6}$  Meters for  $\pi^0$  in the present process.

### $\sigma_\gamma$ in $\pi^0$ decay

The detection process of the photon is governed by its reaction with the atoms and the following coherent transitions by which electronic signals emerge in the detector. They occur within finite spatial area occupied by the wavefunctions in solid. The transition amplitude of the photon is described by the wave packet of this size. Thus  $\sigma_\gamma$  represents the spatial size of the electron wavefunction in the configuration space that the photon interacts with. The initial process depends on the energy. In the energy 0.5 GeV, majority of the events are the pair production due to nucleus electric field. Accordingly,  $\sigma_\gamma = \frac{s_\gamma}{m_\pi^2}$ , where  $s_\gamma \leq 1$ , and  $s_\gamma = 0.5$  is used for a following estimation.

$\sigma_\gamma$  and  $T_i$  derived from  $\sigma_i$  govern the magnitude of  $P^{(d)}$ . For high energy colliding beam experiments, the sizes of the positron and the electron are determined by the spatial size of the electron wavefunction in matter.  $T_i = 10^{-14}$  seconds from the relaxation time, and  $\tau = 10^{-16}$  seconds.

At the time interval,  $T \gg \tau = \frac{1}{\Gamma}$ , the ratio  $T_i\Gamma$  becomes  $\frac{T_i}{\tau}$ . Now,  $c\tau$  is  $10^{-8}$  meter. Accordingly the ratio  $\frac{T_i}{\tau} m_\pi^2 \sigma_\gamma \frac{1}{64} = \frac{10^{-14}}{10^{-16}} \times 0.5 \times \frac{1}{64} = 0.8$ . From this value the probability that one of the photon is in the energy range around the central energy  $E_\gamma^0$ ,  $\frac{E_\gamma - E_\gamma^0}{E_\gamma^0} \leq 0.1$  is about 10 per cent. This would be consistent with the current uncertainty of the neutral pion's average lifetime.

### 2. Sizes of wave functions : $\bar{e}$

#### $\sigma_{e^+}$

First we study the spatial size of the positron wave packet for a process that the gamma from the positron annihilation is measured.  $^{22}\text{Na}$  is at rest and bound in matter. The spatial extension of  $^{22}\text{Na}$ 's wavefunction in the configuration space would be  $\frac{1}{2000}$  of the electron wavefunction from the ratio of the masses. The positron emitted from  $^{22}\text{Na}$  decay has this size in the direction perpendicular to its momentum, and that in the parallel direction can be much longer. This loses the energy in matter in average  $10^{-12}$  second [30]. Hence the time

interval in which the positron wavefunction keeps the coherence or the average relaxation time is  $10^{-12}$  second.

The wave packet size for a detected positron is estimated based on the used detector. When a plastic scintillator in which Benzen is used, the spatial size of the Benzen molecule, around 1 nano meter, shows the positron wave packet size.

$$\sigma_{Ps}$$

Positronium are formed in porus material and decays there. The size of the porus determines an effective size of the interaction area, and determines the time interval of the transition amplitude.

### $\sigma_\gamma$ in positron annihilation

The dominant process of the photon with matter in the detector in this energy region, around a few hundreds KeV, is the photo-electric effect, in which the photon excites the atom. The relevant spatial size is the size of atom, which is characterized by  $\pi \times (\frac{a_\infty}{2})^2$ , where  $a_B = \frac{1}{m_e \alpha}$  is the Bohr radius. Excited atoms make successive transitions and produce many photons, electrons and ions of low energy. These processes are expressed by the time-dependent Schroedinger equation which describe electrons, photons and ions. These states are expressed by the wavefunctions of finite spatial extensions, wave packets. The size of coherent area of these wave functions would be of order few atomic sizes, due to decoherence caused by many atoms. The wave packet size,  $\sigma_\gamma$  of the photon may be of a few atomic sizes. The parameters may depend on the detector, [31, 32].

### B. Boundary regions

The wave functions of the electron and positron overlap at the boundary region of the matter, and their annihilation takes place. The area is large, and the events increases in porus material. The porus size determines an effective size of the area and the time interval of the transition. The transition amplitudes and probabilities depend on these sizes. That is used in the positron experiments.

For experiments that use small powders, electrons are inside of the small region, and the interaction takes place in the inside or at the boundary region. The transition amplitudes and probabilities depend on these sizes.

### C. Energy resolution

An idealistic detector that detects and gives an energy of a particle or a wave directly does not exist. For its measurement, signals caused by its reactions with matter are read first and is converted to the energy using a conversion rule justified by other processes. The energy is measured within finite uncertainty. This is the energy resolution, and all the detector have the finite energy resolution. This causes an experimental uncertainty. The energy resolution,  $\sigma(E)$ , has various origins such as a statistical one and an intrinsic one. That is written as

$$\sigma(E) = \sigma_{statitics}(E) + \sigma_{intrinsic}(E), \quad (18)$$

where  $\sigma_{statitics}(E)$  is determined normally from Poisson statistics and other is written as  $\sigma_{intrinsic}(E)$ , in which an effect due to the finite size of wavefunctions, Eq.(5), is included. The former depends on the detector's type, and the latter does not and has universal properties regardless of detector type. In scintillation detector, an electric signal of a  $\gamma$ -ray is obtained according to the number of the scintillation photons  $N$ , and the energy resolution,  $\sigma_{statitics}(E)$ , is given by

$$\sigma_{statitics}(E) = 2.35\sqrt{\frac{F}{N}}E, \quad (19)$$

where  $N$  is a number of the sample and  $F$  is a correction factor, the Fano-factor. For NaI(Tl),  $F = 1$ , and  $\sigma_{statitics}(E)/\langle E \rangle$  is around 5 – 10 per cent, and the energy resolution is 25 – 50 keV for the energy 500 keV. Ge detector is of different mechanism of much smaller statistical uncertainty, due to the small  $F$  and large  $N$ . The distribution around the central value decreases exponentially with  $E$ .

The wave-packet size determined by the size of the atom is  $\pi(10^{-10})^2 \text{ M}^2$  and should be almost the same in NaI(Tl) and Ge detectors, and leads to the energy uncertainty,  $\sigma_{intrinsic}(E) = 1 \text{ keV}$ . Accordingly in the NaI,  $\sigma_{statitics}(E)$  is the dominant one and  $\sigma_{intrinsic}(E)$  is negligible, but in Ge detector,  $\sigma_{intrinsic}(E)$  shares the substantial part.

### D. Energy distribution

The energy distributions of the bulk term and the boundary term are very different. That from  $\Gamma$  for the plane waves under ASI is proportional to  $\delta(E_i - E_f)$ , but for the wave packets

that behaves as  $e^{-\left(\frac{\delta\omega}{\sigma(E)}\right)^2}$ , where the width is of universal nature and behaves differently from those of statistical one. That of  $P^{(d)}$  decreases in  $E^{-n}$ , where  $n \geq 0$  depends on the decay dynamics.  $P^{(d)}$  can be identified easily in the energy region  $E \gg \sigma(E)$  if the relative fraction over  $\Gamma T$  is of substantial magnitude of the order  $10^{-3}$  or larger, even with the detector of large energy resolution. Despite of large energy resolution, NaI(Tl) scintillator is useful for the confirmation of  $P^{(d)}$ . The detector of much smaller resolution such as the Ge detector is also useful.

## V. EXPERIMENTAL CONFIRMATIONS

As  $P^{(d)}$  possesses many unusual properties, phenomena originated from  $P^{(d)}$  reveal intriguing properties. By detecting these events,  $P^{(d)}$  can be confirmed.  $\Gamma$  has been well established, and phenomena of  $\Gamma$  origin have been understood precisely with a help of numerical methods. They are compared with the data from the natural phenomena and observations. If clear disagreements are found, and if it is resolved by  $P^{(d)}$ , this may confirm  $P^{(d)}$ .

### A. Magnitude of $P^{(d)}$

A magnitude of  $P^{(d)}$  for para-positronium decay,  $P^{(d)}(pp)$ , and direct annihilation,  $P^{(d)}(da)$ , is estimated and given in Figure. They depend on the size and shape of the wave packets. We use the value  $\sigma_\gamma > 10^{-20}\text{m}^2$ , and the Gaussian wave function and power law wave function, and find

$$\begin{aligned} P^{(d)}(pp) &= 10^{-12} ; \text{Gaussian WF} \\ &= 3 \times 10^{-4} \text{ Power law WF} \\ P^{(d)}(da) &= 2 \times 10^{-6} ; \text{Gaussian WF} \\ &= 3 \times 10^{-4} ; \text{Power law WF.} \end{aligned}$$

At the moment we are not aware of the precise shape and size of the wave function. Light scattering may be useful for a study of the wave function [24].

The photon distribution is modified by  $P^{(d)}$  in the positron annihilation and positronium decay. The high energy side is not affected by the modified energy by the Compton scatterings, which is not true on the low energy side. By measuring multiple coincident photons

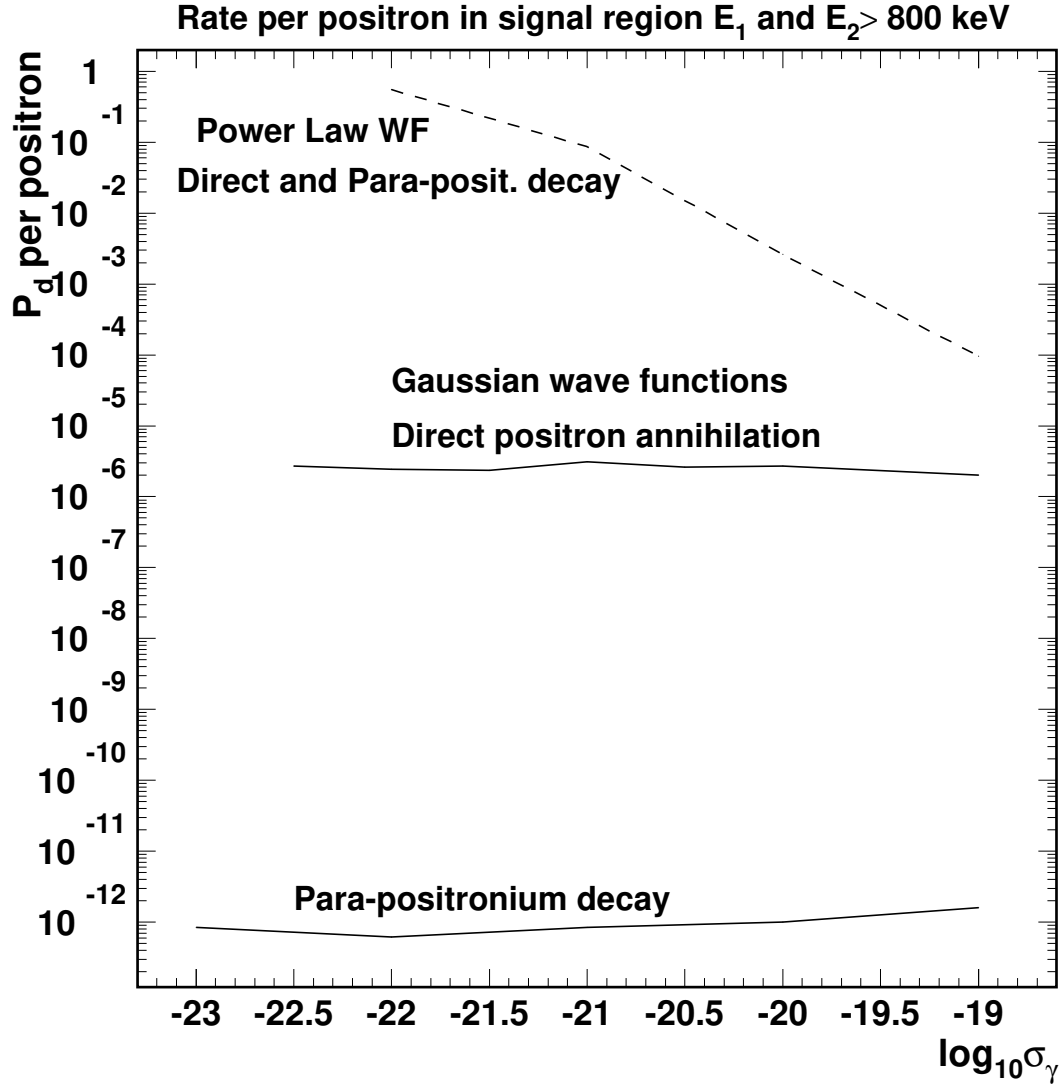


FIG. 1. The variation of the expected ratio of events per stopping positron in silica with  $\sigma_\gamma$  for different assumed situations. The upper curve shows the ratio if direct wave functions are dominant. The middle curve shows the ratio if direct annihilation dominates and the lower curve if the annihilation is dominantly through the decay of para-positronium.

in the high energy regions, clear signals may be obtained. Although accidental coincident events may contribute, the separation of them can be made and events of  $P^{(d)}$  origin in the data is estimated. It is our expectation that with  $10^8$  events of the positron annihilation a confirmation of  $P^d$  could be in scope.

GEANT4[33] is a simulation program that includes the transition probability and the detector performance. The probabilities derived from the golden rule are employed. Hence this is quite useful for analyzing the natural phenomena including the detector's response and backgrounds. Comparing the events derived from the golden rule of the standard theory with the observations, we are able to see if a non-standard component is included.

### B. Backgrounds from decay ( annihilation ) in flight

The signals from the decay or the annihilation in flight are in energy regions different from those at rest and give background. Positron loses its energy in insulator in pico seconds [34], and stops. A photon produced before the stop has an energy higher than  $m_e$  and its contribution is estimated in two steps.

The average positron lifetime, due to the annihilation or the decay is, 100-500 pico seconds, which depends on various conditions. Hereafter we use 200 pico seconds for the average life time and 2 pico second for the thermalization time. The annihilation events of the positron in flight over that at rest is less than the ratio,  $\frac{2}{200} = 10^{-2}$ . The experimental value seems to be less than  $10^{-3}$  or  $10^{-4}$  [35]. Among the events of energy  $E_1 + E_2 > 2m_e c^2$ , a fraction in the energy region  $E_1 + E_2 - 2m_e c^2 \geq 3\sigma E$ , where  $\sigma E$  is the width of NaI(Tl) detector, is obtained as  $\frac{1}{230}$  from Bethe's formula [36]. A further suppression factor  $\frac{1}{10}$  is multiplied due to a specific configuration of the detector setup of the present experiment. Combining these numbers, the fraction is  $0.43 \times 10^{-6}$  or  $0.43 \times 10^{-7}$ . This gives the magnitude of the background from the inflight annihilation, is less than  $10^{-6}$ .

### C. Uncertainties

Possible sources of uncertainties and ambiguities are matter effects, accidental coincident events (double hits), and environmental gammas.

The photon spectrum in the high energy region is not modified by Moeller scattering, photo-electric effect, the Compton effect, and the pair production. Accordingly the matter effects are irrelevant. The environmental gammas or those of cosmic ray origins are avoided by selecting coincident events of multiple gammas. In two gamma's case, the coincidence between one gamma from Ne radiative decay and another from the positron annihilation

are taken. In three gammas case, the coincidence between one gamma from  $^{21}\text{Ne}^*$  radiative decay and two photons from the positron annihilation are taken. In these multiple coincident events, there remain accidental coincident events (double hits). Because their strength depends upon the initial positron flux and the spectrum has different momentum dependence than the signal from  $P^{(d)}$ , it is possible to disentangle them following Appendix B.

#### D. Related processes

Para-positronium decays is included in the text. Other spin component, Orth-Positronium, may be used for  $P^d \neq 0$  test. However, Orth-Positronium has much longer life-time and  $P^{(d)}$  becomes much smaller. Its effect is difficult to observe experimentally.  $P^{(d)}$  in nuclear's gamma and beta decays become also sizable, and can be non-vanishing even in processes of  $\Gamma = 0$ . Various selection rules are valid only to  $\Gamma$ , but to  $P^{(d)}$ . A role of  $P^{(d)}$  is important then.

## VI. SUMMARY AND PROSPECTS

$P^{(d)}$  would be confirmed from the photon's distributions experimentally.

(1) The energies of the photons in the positron annihilation at rest from the golden rule satisfy  $E_{\gamma_1} + E_{\gamma_2} = 2m_e$ , whereas those from  $P^{(d)}$  satisfy  $E_{\gamma_1} + E_{\gamma_2} < 2m_e$  or  $E_{\gamma_1} + E_{\gamma_2} > 2m_e$ . The photon loses its energy by the Compton scattering, and that produced by the golden rule can be detected in the former region, but not in the latter region. The events of the energies  $E_{\gamma_1} + E_{\gamma_2} > m_e$  are generated only by  $P^{(d)}$ , and may be worthwhile for its confirmation.

(2) For the neutral pion, our finding  $P^{(d)} \approx O(0.8)$  suggest that for the analysis  $P^{(d)}$  must be implemented. The previous large uncertainty of about 10 per cent in the life time would be due to  $P^{(d)}$ , and will be reduced in an analysis that includes  $P^{(d)}$ .

(3) Tagging  $\pi^+$  and  $\pi^-$  in the process  $e + \bar{e} \rightarrow \phi, \phi \rightarrow \pi^+ + \pi^- + \pi^0$ , the  $\pi^0$  momentum is determined, and the photon spectrum is computed. Due to  $P^{(d)}$ , this spectrum deviates from the golden rule. If the deviation is observed,  $P^{(d)}$  will be confirmed.

(4) Many-body wave functions of  $\delta E = E_{initial} - (E_{\gamma_1} + E_{\gamma_2}) \neq 0$  have interaction energies, which are independent of the frequency of each wave. This leads an extra component to the energy momentum tensor in addition to those proportional to the frequencies. Normal

detection processes measure the wave's frequencies, but these interaction energies. Accordingly, this corresponds to an invisible energy. This state may be considered as a kind of halo.

(5) Once the confirmation of  $P^d$  is made, (a) methods to reduce current uncertainties in the experiments and (b) mechanisms to solve current puzzling phenomena will be found.

## Acknowledgments

This work was partially supported by a Grant-in-Aid for Scientific Research ( Grant No. 24340043). The authors thank Dr. K. Hayasaka, Dr. K. Oda, and Mr. H. Nakatsuka for useful discussions.

- 
- [1] P. A. M. Dirac. Pro. R. Soc. Lond. A 114, 243 (1927).
  - [2] L. I. Schiff. *Quantum Mechanics* (McGRAW-Hill Book COMPANY, Inc. New York, 1955).
  - [3] K. Ishikawa and K. Oda, Prog. Theor. Exp. Phys.123B01, doi:10.1093/ptep/pty127(2018). arXiv:1809.04285[hep-ph],
  - [4] C. Patrignani *et al.* [Particle Data Group], Chi. Phys. C , **40**, 100001 (2016) and 2017 update.
  - [5] H.Fukuda and Y.Miyamoto, Prog.Theor. Phys.**4**,235(1949); **4**,347(1949)
  - [6] J.Steinberger, Phys. Rev.**76**1180(1949)
  - [7] S.Adler, Phys.Rev.**177**,2426(1969)
  - [8] J. Bell and R.Jackiw, Nuovo Cimento **A60**,47(1969)
  - [9] A.M. Bernstein and Barry.R.Holstein, Rev.Mod.Phys. **85**,49,(2013)
  - [10] S.G.Stueckelberg, Phys. Rev. **81**, 130,(1951).
  - [11] M. L. Goldberger and Kenneth M. Watson, *Collision Theory* (John Wiley & Sons, Inc. New York, 1965).
  - [12] R. G. Newton, *Scattering Theory of Waves and Particles* (Springer-Verlag, New York, 1982).
  - [13] J. R. Taylor, *Scattering Theory: The Quantum Theory of non-relativistic Collisions* (Dover Publications, New York, 2006).
  - [14] K. Ishikawa and T. Shimomura, Prog. Theor. Phys. **114**, 1201 (2005) [hep-ph/0508303].
  - [15] K. Ishikawa and Y. Tobita. Prog. Theor. Exp. Phys. 073B02, doi:10.1093/ptep/ptt049 (2013).

- [16] K. Ishikawa and Y. Tobita. *Ann. of Phys.* 344, 118(2014).doi:10.1016/j.aop.2014.02.007
- [17] K. Ishikawa, T.Tajima, and Y. Tobita. *Prog. Theor. Exp. Phys.* 2015, 013B02, (2015), doi:10.1093/ptep/ptu168.
- [18] R. Peierls. *Surprises in Theoretical Physics* (Princeton University Press, New Jersey 1979) p.121
- [19] H. Lehman, K. Symanzik, and W. Zimmermann, *Il Nuovo Cimento* (1955-1965). **1**, 205 (1955).
- [20] F. Low, *Phys. Rev.* **97**, 1392 (1955).
- [21] V. Weisskopf and E. P. Wigner, *Z. Phys.* **63** (1930) 54.
- [22] V. Weisskopf and E. Wigner, *Z. Phys.* **65** (1930) 18.
- [23] J. Liu, *Phys. Rev.* D44.2879 (1991)
- [24] Raman scattering experiment has seen anomalous signals. Private communications from Professor.M. Takesada.
- [25] L. Stodolsky. *Phys. Rev.* **D58**, 036006 (1998) [hep-ph/9802387]. This work and other works studied the neutrino oscillation amplitude within the golden rule in the wave packet formalism. See the following two papers for recent references.
- [26] H. J. Lipkin. *Phys. Lett.* **B642**, 366 (2006) [hep-ph/0505141].
- [27] E. K. Akhmedov. *JHEP.* **0709**, 116 (2007) [arXiv:0706.1216 [hep-ph]].
- [28] K. Ishikawa and Y. Tobita. *Prog. Theor. Phys.* **122**, 1111 (2009) [arXiv:0906.3938[quant-ph]].
- [29] N.Maeda, T.Yabuki, Y.Tobita, and K. Ishikawa, *Prog. Theor. Exp. Phys.* 053J01, doi:10.1093/ptep/ptx066 (2017).
- [30] F. Rohrich and B.C. Carson, *Phys.Rev.*93,38(1954)
- [31] I. Hossain, N. sharip, and K.K.Viswanathan, *Scientific Research and Essays*, 7(1), 86-89(2012)
- [32] M.Moszyski, et al. , *Nuclear Ins. and Methods in Physics Research A* 484, 259-269, (2002)
- [33] S. Agostinelli et al. , “GREANT4: A simulation toolkit”, *Nucl. Instrum. Meth. A.* 506 (2003) 250.
- [34] S.Tanuma,C. J. Powell, and D.R.Penn, ‘*Jouenal of Applied Physics* 103, 063707(2008)
- [35] J. Cizek et al., *Journal of Physics: Conference Series* 505 (2014) 012043
- [36] H. A. Bethe, *Proceedings of the Royal Society of London, Series.A, Mathematical and Physical Sciences*, Vol 150, No.869, 129-141

## APPENDIX

### Appendix A: Free positron annihilation

#### 1. Amplitude

An amplitude for a free positron annihilation is

$$M = \int_0^T dt_1 \int d^3x_1 \int_0^{t_1} dt_2 d^3x_2 \langle \gamma_1, \gamma_2 | H_{int}(x_1) H_{int}(x_2) | e, \bar{e} \rangle, \quad (\text{A1})$$

$$= \frac{1}{2} \int_0^T dt_1 \int_0^{t_1} dt_2 d^3x_1 d^3x_2 \langle \gamma_1, \gamma_2 | T(H_{int}(x_1) H_{int}(x_2)) | e, \bar{e} \rangle, \quad (\text{A2})$$

where  $H_{int}(x)$  is the interaction part of QED and the initial and final states are wave packets, and

$$T(H_{int}(t_1) H_{int}(t_2)) = \theta(t_1 - t_2) H_{int}(t_1) H_{int}(t_2) + \theta(t_2 - t_1) H_{int}(t_2) H_{int}(t_1). \quad (\text{A3})$$

Applying the Wick's theorem,

$$\begin{aligned} M &= \sum :: \gamma_\mu S_F(x_1 - x_2) \gamma_\nu + \dots \quad (\text{A4}) \\ &= \bar{u}(p_1) [\gamma\epsilon(k_1) \frac{\gamma(p_1 - k_1) + m_e}{(p_1 - k_1)^2 - m_e^2} \gamma\epsilon(k_2) + \gamma\epsilon(k_2) \frac{\gamma(p_1 - k_2) + m_e}{(p_1 - k_2)^2 - m_e^2} \gamma\epsilon(k_1)] v(p_2) \\ &= -\bar{u}(p_1) \left[ \frac{\gamma k_1 \gamma\epsilon(k_1) \epsilon(k_2) + 2\epsilon(k_1) p_1 \gamma\epsilon(k_2)}{2p_1 k_1} + \frac{\gamma k_2 \gamma\epsilon(k_2) \gamma\epsilon(k_1) + 2\epsilon(k_2) p_1 \gamma\epsilon(k_1)}{2p_1 k_2} \right] v(p_2) \quad (\text{A5}) \end{aligned}$$

where

$$\bar{u}(p_1) \gamma\epsilon(k_1) (\gamma p_1 + m_e) = 2\epsilon(k_1) p_1 \bar{u}(p_1) \quad (\text{A6})$$

and the similar one for the  $v(p_2)$  were substituted. For  $p_1 = (m, o), p_2 = (m, o)$  it follows

$$\sum_{spin} |M|^2 = \frac{8}{m_e^2} \left[ 1 + \frac{1}{4} (1 - \cos \theta) + \frac{1}{2} \left( \frac{m}{k_1^0} + \frac{m}{k_2^0} \right) \right]. \quad (\text{A7})$$

Note that this is slightly different from that of the positronium decays.

#### 2. Boundary in space and time

##### a. Amplitude

In scatterings in laboratory frame where the target is composed of small particles of the volume  $L^3$ , the momentum dependent amplitudes in the bulk and boundary terms, of

Eq.(15) in August 25 version are replaced with

$$M_{bulk} = \sqrt{2\pi\sigma_t} e^{-\frac{\sigma_t}{2}(\delta\omega)^2} (2\pi\sigma_s)^{3/2} e^{-\frac{\sigma_s}{2}(\delta\vec{p})^2} \theta(\vec{X}_\gamma, volume) \quad (A8)$$

$$M_{boundary(t)} = \sqrt{\frac{2\sigma_t}{\pi}} \frac{1}{-i\sqrt{\sigma_t}\delta\omega + 1} (2\pi\sigma_s)^{3/2} e^{-\frac{\sigma_s}{2}(\delta\vec{p})^2} \theta(\vec{X}_\gamma, b_t) \quad (A9)$$

$$M_{boundary(s)} = \sqrt{\frac{2\sigma_t}{\pi}} \frac{1}{-i\sqrt{\sigma_t}\delta\omega + 1} (2\pi\sigma_s)^{2/2} \sqrt{\frac{2\sigma_s}{\pi}} \times \theta(\vec{X}_\gamma, b_{(t,s)}) \\ \left[ \frac{1}{-i\sqrt{\sigma_s}\delta p_z + 1} e^{-\frac{\sigma_s}{2}((\delta\vec{p}_x)^2 + (\delta\vec{p}_y)^2)} + (z, x, y) \rightarrow (x, y, z), (y, z, x) \right]. \quad (A10)$$

where  $\theta(\vec{X}_\gamma, volume)$ ,  $\theta(\vec{X}_\gamma, b_t)$ , and  $\theta(\vec{X}_\gamma, b_{(t,s)})$  show that the intersection of trajectories are in the inside of the volume  $L^3$ , in the boundary in time, and in the boundary in space and time.

The momentum dependent term in the bulk, Eq.(21), and the boundary term in time, Eq.(22), lead the probability of the same form as before,

$$|G_{bulk}(\delta\omega)|^2 = (\sqrt{2\pi\sigma_t} e^{-\frac{\sigma_t}{2}(\delta\omega)^2})^2 (2\pi\sigma_s)^3 \quad (A11) \\ |G_{boundary(t)}(\delta\omega)|^2 = \left| \sqrt{\frac{2\sigma_t}{\pi}} \frac{1}{-i\sqrt{\sigma_t}\delta\omega + 1} \right|^2 (2\pi\sigma_s)^3$$

but the space-boundary term

$$e^{-\sigma_s(\delta\vec{p})^2} |G_{boundary(s)}(\delta\omega)|^2 = \left( \sqrt{\frac{2\sigma_t}{\pi}} \frac{1}{|-i\sqrt{\sigma_t}\delta\omega + 1|} \sqrt{\frac{2\sigma_s}{\pi}} (2\pi\sigma_s) \right)^2 \\ \times \left[ \left| \frac{1}{-i\sqrt{\sigma_s}\delta p_z + 1} \right|^2 e^{-\sigma_s((\delta\vec{p}_x)^2 + (\delta\vec{p}_y)^2)} + |(x, y, z)|^2 + |(y, z, x)|^2 \right]. \quad (A12)$$

is different. The momentum dependence of the bulk term and that of the time-boundary are spherically symmetric as before but that of the space-boundary is asymmetric.

### 3. Normalization of Probability: summation over the positions

The integration over the positions  $\vec{X}_{\gamma_i}$ , and over the position  $\vec{X}_{e+}$  in the region of  $L^3$  and the time interval  $T$ , and for the boundary of the width  $\sqrt{2\sigma_t}$  and  $\sqrt{2\sigma_s}$  are,

$$\int d\vec{X}_{e+} \int \frac{d\vec{X}_{\gamma_1} d\vec{X}_{\gamma_2}}{(2\pi)^6} e^{-2R(\vec{X}_{\gamma_i})} \theta(\vec{X}_{\gamma}, \text{volume}) = TL^3 \quad (\text{A13})$$

$$\int d\vec{X}_{e+} \int \frac{d\vec{X}_{\gamma_1} d\vec{X}_{\gamma_2}}{(2\pi)^6} e^{-2R(\vec{X}_{\gamma_i})} \theta(\vec{X}_{\gamma}, b_t) = \frac{\sqrt{2\sigma_t}}{T} (TL^3) \quad (\text{A14})$$

$$\int d\vec{X}_{e+} \int \frac{d\vec{X}_{\gamma_1} d\vec{X}_{\gamma_2}}{(2\pi)^6} e^{-2R(\vec{X}_{\gamma_i})} \theta(\vec{X}_{\gamma}, b_{s,t}) = \frac{\sqrt{2\sigma_t 2\sigma_s}}{TL} (TL^3) \quad (\text{A15})$$

Substituting these, we have the momentum distribution

$$\begin{aligned} \frac{1}{TL^3} \frac{dP}{d^3k_1 d^3k_2} &= \frac{2}{m^2} \left( 1 + \frac{1}{4}(1 - \cos \theta) + \frac{1}{2} \left( \frac{m}{E_{\gamma_1}} + \frac{m}{E_{\gamma_2}} \right) \right) \\ & \left[ e^{-\sigma_s(\delta P)^2} (P_0^{bulk} |G_{bulk}(\delta\omega)|^2 + P_0^{bt} |G_{boundary(t)}(\delta\omega)|^2) \right. \\ & \left. + P_0^{bs} e^{-\sigma_s(\delta P)^2} |G_{boundary(s)}(\delta\omega)|^2 \right], \end{aligned} \quad (\text{A16})$$

where Eqs.(A22) and (A12) are substituted, and

$$P_0^{bulk} = (E_{e+} E_{\gamma_1} E_{\gamma_2})^{-1} C \quad \text{bulk}, \quad (\text{A17})$$

$$P_0^{b(t)} = (E_{e+} E_{\gamma_1} E_{\gamma_2})^{-1} C \frac{\sqrt{2\sigma_t}}{T} \quad \text{boundary in time}, \quad (\text{A18})$$

$$P_0^{b(s)} = (E_{e+} E_{\gamma_1} E_{\gamma_2})^{-1} C \frac{\sqrt{2\sigma_t 2\sigma_s}}{TL} \quad \text{boundary in space}, \quad (\text{A19})$$

where  $C$  is the constant. In the present situation, the target is composed of silica particles of  $L = 7$  nano meter, and it is reasonable to assume  $E_{e+} = m_e(1 \pm \frac{1}{10})$ ,  $\frac{\sqrt{2\sigma_s}}{L}$ ,  $\frac{\sqrt{2\sigma_t}}{T} \approx \frac{1}{10} - \frac{1}{100}$ . The spectrum of the boundary term is of the universal form but its magnitude has uncertainties due to the uncertainties on the wave packets. This ambiguity could be studied by a light scattering of the silica powder.

### 4. Non-Gaussian wave packet

Function  $e^{-\mu r}$ , where  $r = |\vec{x}|$  and  $\mu$  is a constant, decreases rapidly at large distance  $r$  but has a singularity at  $r = 0$ . Its Fourier transform is  $\frac{1}{(p^2 + \mu^2)^2}$ , and is decreasing slowly in the momentum. Accordingly, the wave packet of this form leads a probability different from the Gaussian one. This is studied hereafter.

a. *Amplitude*

For the non-Gaussian wave packets, the momentum dependent amplitudes in the bulk and boundary terms are

$$M_{bulk} = f_0 \frac{\frac{2}{t_0}}{\omega^2 + (\frac{1}{t_0})^2} \times f_0 8\pi \frac{1}{r_0} \frac{1}{((\frac{1}{r_0})^2 + (\delta\vec{p})^2)^2} \theta(\vec{X}_\gamma, volume) \quad (A20)$$

$$M_{boundary(t)} = f_0 \frac{1}{i\omega + \frac{1}{t_0}} \times f_0 8\pi \frac{1}{r_0} \frac{1}{((\frac{1}{r_0})^2 + (\delta\vec{p})^2)^2} \theta(\vec{X}_\gamma, b_t), \quad (A21)$$

where  $f_0 = \frac{1}{\sqrt{\pi r_0^3}}$ , and  $t_0$  and  $r_0$  are determined from the size of the Coulomb wave function and for NaI are given at the end of this Appendix. These lead the probability of the same form as before,

$$|G_{bulk}(\delta\omega, \delta\vec{p})|^2 = [f_0 \frac{\frac{2}{t_0}}{\omega^2 + (\frac{1}{t_0})^2} \times f_0 8\pi \frac{1}{r_0} \frac{1}{((\frac{1}{r_0})^2 + (\delta\vec{p})^2)^2}]^2, \quad (A22)$$

$$|G_{boundary(t)}(\delta\omega, \delta\vec{p})|^2 = [f_0 \frac{1}{i\omega + \frac{1}{t_0}} \times f_0 8\pi \frac{1}{r_0} \frac{1}{((\frac{1}{r_0})^2 + (\delta\vec{p})^2)^2}]^2.$$

The integration over the positions  $\vec{X}_\gamma$ , and over the position  $\vec{X}_{e+}$  are also the same as before.

We have the momentum distribution

$$\begin{aligned} \frac{1}{TL^3} \frac{dP}{d^3k_1 d^3k_2} &= \frac{2}{m^2} (1 + \frac{1}{4}(1 - \cos\theta) + \frac{1}{2}(\frac{m}{E_{\gamma_1}} + \frac{m}{E_{\gamma_2}})) \\ &\times [(P_0^{bulk} |G_{bulk}(\delta\omega, \delta\vec{p})|^2 + P_0^{bt} |G_{boundary(t)}(\delta\omega, \delta\vec{p})|^2)] \end{aligned} \quad (A23)$$

where Eqs.(A22) and (A12) are substituted, and

$$\begin{aligned} P_0^{bulk} &= (E_{e+} E_{\gamma_1} E_{\gamma_2})^{-1} C_{Coul} && \text{bulk,} \\ P_0^{b(t)} &= (E_{e+} E_{\gamma_1} E_{\gamma_2})^{-1} C_{Coul} \frac{\sqrt{2\sigma_t}}{T} && \text{boundary,} \end{aligned} \quad (A24)$$

where  $C_{Coul}$  is a constant which is related with  $C$ , and  $r_0 = \frac{\sqrt{\sigma_s}}{50}$  and  $t_0 = \frac{\sqrt{\sigma_t}}{50}$ . We leave  $C_{Coul}$  as a parameter for a while.

## Appendix B: Duplicate (accidentally coincident and pile-up) events

Suppose the probability is a sum of duplicate (accidental coincident and pile-up) events and  $P^{(d)}$  events

$$f(p_1, p_2) = c_0 g(p_1) g(p_2) + g(p_1, p_2) \quad (B1)$$

where  $g(p_1)$  and  $g(p_1, p_2)$  are known theoretically, but  $c_0$  in experiments is unknown. Define an error function

$$\begin{aligned}
I_{error}(c) &= \int dp_1 dp_2 (f_{exp}(p_1, p_2) - cg(p_1)g(p_2))^2 \quad (\text{B2}) \\
&= \int dp_1 dp_2 [(c - c_0)^2 (g(p_1)g(p_2))^2 + (g(p_1, p_2))^2 - 2(c - c_0)g(p_1)g(p_1, p_2)g(p_2)] \\
&= (c - c_0)^2 A_2 - 2(c - c_0)A_1 + A_0 = A_2(c - \tilde{c}_0)^2 + A_0 - A_1^2/A_2
\end{aligned}$$

$$A_2 = \int dp_1 dp_2 (g(p_1)g(p_2))^2, A_1 = \int dp_1 dp_2 g(p_1)g(p_1, p_2)g(p_2), A_0 = \int dp_1 dp_2 (g(p_1, p_2))^2$$

Plot  $I_{error}(c)$  as a function of  $c$  and obtain the minimum value  $D = A_0 - A_1^2/A_2$ ,

$$D = -[\int dp_1 dp_2 g(p_1)g(p_1, p_2)g(p_2)]^2 / [\int dp_1 dp_2 (g(p_1)g(p_2))^2] + \int dp_1 dp_2 g(p_1, p_2)^2 \quad (\text{B4})$$

$P^{(d)} = 0$ ,  $g(p_1, p_2) = 0$ , and  $D = 0$ , for  $P^{(d)} \neq 0$ ,  $g(p_1, p_2) > 0$ , and  $D > 0$ . Experimental determination of  $D > 0$  may be feasible.